Published in final edited form as:
Oncogene. 2009 June 11; 28(23): 2289–2298. doi:10.1038/onc.2009.95.

Melanocytic nevus-like hyperplasia and melanoma in transgenic BRAFV600E mice

VK Goel[1], **N Ibrahim**[1], **G Jiang**[1], **M Singhal**[1], **S Fee**[2], **T Flotte**[2], **S Westmoreland**[3], **FS Haluska**[2], **PW Hinds**[1], and **FG Haluska**[1]

[1] Molecular Oncology Research Institute, Tufts New England Medical Center, Boston, MA, USA

[2] Massachusetts General Hospital, Boston, MA, USA

[3] New England Primate Research Center, Harvard Medical School, Boston, MA, USA

Abstract

BRAF, a cellular oncogene and effector of RAS-mediated signaling, is activated by mutation in ~60% of melano-mas. Most of these mutations consist of a V600E substitution resulting in constitutive kinase activation. Mutant BRAF thus represents an important therapeutic target in melanoma. In an effort to produce a pre-clinical model of mutant BRAF function in melanoma, we have generated a mouse expressing *BRAF* V600E targeted to melanocytes. We show that in these transgenic mice, widespread benign melanocytic hyperplasia with histolo-gical features of nevi occurs, with biochemical evidence of senescence. Melanocytic hyperplasia progresses to overt melanoma with an incidence dependent on *BRAF* expression levels. Melanomas show *CDKN2A* loss, and genetic disruption of the *CDKN2A* locus greatly enhances melanoma formation, consistent with collaboration between BRAF activation and CDKN2A loss suggested from studies of human melanoma. The development of melanoma also involves activation of the Mapk and Akt signaling pathways and loss of senescence, findings that faithfully recapitulate those seen in human melanomas. This murine model of mutant BRAF-induced melanoma formation thus provides an important tool for identifying further genetic alterations that cooperates with BRAF and that may be useful in enhancing susceptibility to BRAF-targeted therapeutics in melanoma.

Keywords

BRAF; p53; CDKN2A; AKT; melanoma; senescence

Introduction

The most prevalent oncogenic mutations that pose a potential therapeutic target in human melanoma occur in BRAF (Pollock and Meltzer, 2002). This protein is a serine–threonine specific protein kinase that is activated by RAS and that functions to transduce signals intracellularly. BRAF mutations have been detected in 60–70% of malignant melanomas and in a variety of other cancer types, including thyroid, lung and colon cancers, with most mutations comprising a single substitution (V600E) that results in constitutive activation of

Correspondence: Dr VK Goel, Molecular Oncology Research Institute, Tufts New England Medical Center, 750 Washington Street, Boston, MA 2111, USA., vkumargoel@gmail.com or Dr FG Haluska, ARIAD Pharmaceuticals, 26 Landsdowne Street, Cambridge, MA 02139-4234, USA. frank.haluska@ARIAD.com.

Conflict of interest

The authors declare no conflict of interest.

Supplementary Information accompanies the paper on the Oncogene website (http://www.nature.com/onc)

the kinase function (Pollock and Meltzer, 2002; Goel *et al.,* 2006). BRAF mutation is not sufficient to induce malignancy: it has been shown that up to 80% of benign nevi carry the same mutation in BRAF as is observed in melanoma (Pollock *et al.,* 2003). Yet the high prevalence of BRAF mutation in this disease, and earlier successes in using small-molecule inhibitors to treat other solid tumors with activating kinase mutations (Lynch *et al.,* 2004), suggests that BRAF is an appealing therapeutic target in melanoma, although in clinical trials initial attempts to target BRAF with the small-molecule inhibitor sorafenib have yielded only rare tumor responses (Bardeesy *et al.,* 2001). The observed mutation rate of *BRAF* in benign nevi, and the small fraction of nevi that transform to melanoma, underscores the fact that genetic changes in addition to those found in BRAF are necessary for the development of overt melanoma. Understanding these additional alterations may be a prerequisite for successful BRAF-targeted treatments.

Perhaps the most important additional genetic changes identified in melanoma are in the *Cdkna2a* locus, which encodes both $p16^{INK4A}$ and $p14^{ARF}$ ($p19^{Arf}$ in the mouse). Germline mutations in $p16^{INK4A}$ confer a familial predisposition for melanoma (Haluska *et al.,* 2006; Laud *et al.,* 2006), and recent findings implicate $p16^{INK4A}$ in the senescent response to oncogene mutation (Gray-Schopfer *et al.,* 2006). In melanocytes, BRAF mutation alone leads to nevus formation with initial cell proliferation and later growth arrest and senescence with concomitant induction of both $p16^{INK4A}$ and senescence-activated &*beta;*-galactosidase (SA-&*beta;*-gal). Subsequent loss of $p16^{INK4A}$ occurs with tumor progression (Michaloglou *et al.,* 2005). Several murine models that introduce activated H-RAS into a background deficient in *Cdkn2a* or $p16^{Ink4a}$ alone support the role of this locus in melanoma development (Chin *et al.,* 1997).

The p53 pathway is also abrogated in melanoma-genesis. Mutations in p53 itself are rare. However, as alternative splicing of the *CDKN2A* mRNA yields two distinct messages, encoding $p16^{INK4A}$ and the p53-modulator $p14^{ARF}$, loss of the locus results in reduction of p53 pathway activity. Recent studies suggest a critical role for the function of $p14^{ARF}$ as a tumor suppressor. It serves to arrest cell cycle progression or promote cell death after oncogenic stimulation, loss of pRb or DNA damage, and participates in the control of p53 through its interaction with the MDM2 protein (Muthusamy *et al.,* 2006; Chang *et al.,* 2007). $p14^{ARF}$ deficiency has been shown to abrogate oncogene-induced senescence and to increase susceptibility to transformation. Loss or mutation of $p14^{ARF}$ facilitates the progression of melanoma, and it is thought that the low frequency of p53 mutations in melanoma is related to the frequent loss of $p14^{ARF}$, which renders p53 mutation or loss superfluous (Castresana *et al.,* 1993). As is the case for $p16^{INK4A}$, murine studies support the role of the p53 pathway in melanoma in studies showing that $p19^{Arf-/-}$/Tyr-Hras and $p53^{-/-}$/Tyr-Hras mutant mice develop melanoma with high penetrance (Bardeesy *et al.,* 2001; Sharpless *et al.,* 2003).

Murine models of the above genetic alterations that incorporate recent findings on BRAF will prove useful in dissecting the common and distinct role of activated signaling and CDKN2A and p53 pathways *in vivo* in the melanocyte lineage. To better understand the biology of BRAF mutation in melanoma and its therapeutic implications, we constructed a mouse model in which the *BRAF* V600E is specifically expressed in melanocytes using the mouse tyrosinase enhancer and promoter. Mice carrying a transgenic mutant BRAF showed benign melanocytic hyperplasia histologically reminiscent of human nevi. We then crossed the *BRAF* V600E transgenic mice with *Cdkn2a*-null (affecting both $p16^{Ink4a}$ and $p19^{Arf}$) and *p53*-null mice. We show here that mice carrying the mutant BRAF allele develop melanoma, and that the genetic features of the melanoma suggest that senescence is overcome concurrent with the loss of $p16^{Ink4a}$ expression, in some cases *Cdkn2a* locus deletion, and activation of Akt. In backgrounds heterozygous for either *Cdkn2a* or *p53* deficiency,

melanoma develops with an enhanced incidence, a shorter latency to tumor formation, and metastases to lung and lymph nodes. This murine system faithfully recapitulates the genetic changes seen in human melanoma.

Results and discussion

Transgenic mutant *BRAF V600E* expression from a Tyr-promoter leads to melanocytic and Schwann cell hyperplasia with evidence of senescence

The mutant *BRAF* expression construct was designed such that the *BRAF V600E* gene, cloned from a human melanoma cell line, was inserted into the vector (pNEB 193) downstream of the murine tyrosinase locus control region (promoter enhancer) (Supplementary Figure 1a). This construct was injected into single-cell embryos of F1 C57BL/J6XCBA mice and the offspring were genotyped by Southern blotting as shown in Figure 1a. Four independent founder lines that expressed the transgene in the germline were propagated for study and the sequence of the transgene was verified. As shown in Figure 1b, RT–PCR showed that the transgene was expressed in the skin and brain and very weakly in the lung (Figure 1b, lanes 2, 6 and 5, respectively), but not in the heart, kidney or liver, with the expression in the skin resulting at least in part from expression in melanocytes (Figure 1b, lanes 14, 15 and 16).

Two founder lines, denoted 470 and 476, were studied in detail. These lines differed in the extent of their phenotype, with line 470 being more penetrant. Real-time RT–PCR examination of the level of *BRAF* V600E transcript expression in the two lines (Figure 1c) found that the level of expression of transgene was three-fold higher in line 470 as compared with line 476, whereas there is no transgene expression in wild-type skin samples. To determine the relative expression levels of the transgene, immunoblotting was carried out to detect both murine endogenous and human exogenous BRAF (which are not distinguishable by available antibodies). The results showed that there were no discernible differences in total BRAF protein (we used total cell lysates from cultured mouse melanocytes and also whole-skin lysate from both wild-type and transgenic animals for the analysis), suggesting the transgenic protein level is low compared with endogenous levels (Figure 1e and Supplementary Figure 1b). Using qRT–PCR, we did not see any difference between wild-type and transgene expression, suggesting transgene expression is low compared with endogenous BRAF. However, we cannot discount the possibility that a small percentage of melanocytes have a high level of expression of the transgene, which in turn drives the neoplastic phenotype.

The phenotype of line 470 compared with C57BL6 is shown in Figure 1d. The animals that carried mutant *BRAF* had hyperpigmented skin, most evident in the ear pinnae and the limbs, their coat color varied from normal to light, their tail was hypertrophied, and the eyes of some animals were small. Gross examination at necropsy (Figure 1d) showed that the dermis is uniformly hyperpigmented.

Histopathology showed that the hyperpigmentation was consequent to a benign melanocytic hyperplasia similar to nevi. Two patterns of melanocytic proliferation were observed. The most prevalent pattern showed abundant spindle cells in the dermis and subcutaneous tissue, frequently termed ‘Schwannian’ differentiation of melanocytes, visualized most prominently in line 470 (Figure 2a, panel 2). The second pattern, more characteristic of the 476 line, showed large nests of epithelioid cells, generally located in the deep dermis and subcutis (Supplementary Figure 2a, panel 4). Both patterns are of melanocytic origins as evident by S-100 staining (data not shown). No mitotic figures were identified in either pattern (data not shown).

The central nervous tissue was involved most prominently in line 470 (Figure 2a, panels 3, 4, 5 and 6). Pigmented spindle cell proliferations were identified in the retro- and peri-bulbar areas of the eye, the meninges, the temporal and parietal bones of the cranium, bone marrow cavity, and in the surrounding soft tissues (Figure 2a, panels 5 and 6). The infiltrative spindle cell tumors were variably pigmented with rare mitoses, and these cells showed neural crest differentiation representing Schwannian differentiation as in the skin (compare Figure 2a, panels 2 and 4). Electron microscopy showed the characteristic lamellar morphology of pigmented cells consistent with Schwann cells (Supplementary Figure 2b). Ultrastructurally there were groups of spindled pigmented cells that exhibited features of Schwannian differentiation, including prominent external lamina with lamina lucida and lamina densa, numerous pinocytotic vesicles, and abundant interdigitating cell processes with infoldings of membranes forming pseudomesaxons around collagen bundles. The presence of melanosomes at varying stages of development showed that these tumor cells are capable of melanogenesis. The majority of these proliferations seem benign; however, the extension into the cortex showed the capacity for at least locally aggressive behavior.

Our observations are consistent with the known expression of tyrosinase in the brain. Tyrosinase transcriptional function has been reported earlier in several regions of the mouse brain, including retinal pigment epithelial cells (Tief *et al.*, 1998). Tyrosinase Cre-recombinase mice made by (Tonks *et al.* 2003) showed that tyrosinase is also expressed in other neural crest and neuroepithelial derived cells. In their mouse model, the reporter gene under the control of the tyrosinase enhancer and promoter is expressed in the glia of the optic nerve (neuroepithelial derived cells), basal forebrain, hippocampus, olfactory bulbs and the granule cell layer of the lateral cerebellum cortex. Functionally, it has been proposed that tyrosinase may serve a role in neuromelanin synthesis within some of these neural tissues (Tief *et al.*, 1998). Indeed, a proportion of catecholaminergic neurons of substantia nigra in tyrosine hydroxylase knockout mice were able, through tyrosinase-mediated pathways, to produce norepinephrine and dopamine at levels of 8 and 2–3% of control mice, respectively.

Examination of the liver, lung, spleen, heart, pancreas, kidney and gastrointestinal tissue showed no involvement

We concentrated on the cutaneous melanocytic phenotype. Immunohistochemistry showed that the transgenic melanocytes expressed moderate levels of pErk1/2 as compared with wild-type skin (compare Figures 2b, panels 1 and 2), but not pAkt (Figure 2b, panel 4), and expression of $p16^{Ink4a}$ (Figure 2b, panel 6), *p53* (Figure 2b, panel 7) and *Pten* (Figure 2b, panel 8) was observed. Wild-type skin showed little p16 expression, which suggests that p16 is induced by mutant BRAF in transgenic skin (Figure 2b, panel 5). The hyperplastic melanocytes also expressed senescence-associated β-galactosidase (*SA-β-gal*), a marker for senescence (Figure 2c, panel 1), and the senescent melanocytes did not form soft agar colonies. The co-expression of mutant BRAF, p16 and SA-*β*-gal suggests a senescence mechanism. Indeed (Michaloglou *et al.* (2005) have shown *in vitro* that *BRAF* V600E expression in melanocytes induces senescence, and that human nevi carrying *BRAF* mutations express SA-*β*-gal. This group and others have also suggested that the senescent mechanism is mediated through $p16^{Ink4a}$ in melanocytes (Sviderskaya *et al.*, 2002; Michaloglou *et al.*, 2005; Gray-Schopfer *et al.*, 2006; Courtois-Cox *et al.*, 2006). Our data are consistent with these reports.

We sought to examine whether these changes are specifically attributable to mutant BRAF, and to understand the biochemical consequences of signaling in these tissues. siRNA specific for the mutant human *BRAF* was introduced into cultured melanocytes from transgenic animals (Figure 1f). As shown, the specific human BRAF V600E specific siRNA, but not irrelevant control siRNA, decreased levels of phosphorylated Mek and Erk (Sharma

et al., 2005), suggesting that the transgene-encoded mutant BRAF is responsible for the altered signaling observed in transgenic mouse skin.

Transgenic animals carrying mutant *BRAF* develop melanoma

Melanomas developed in the animals carrying trans-genic mutant *BRAF* with an incidence dependent on BRAF expression levels, and survival was affected concomitantly (Supplementary Table 1). Figure 3a (panels 1 and 2) shows a melanoma from the 470 line, and a metastasis to a lymph node draining the region. Tumors were located in the dermis, subcutis and soft tissues, and were composed of pigmented epithelioid cells with nuclear pleomorphism and mitotic figures. All melanocytic proliferations showed cytoplasmic and nuclear staining for S100 protein (Figure 3b, panel 2). The benign melanocytic proliferations showed only rare cells staining for Ki-67, constituting <1% of the cells, whereas in the melanomas Ki-67 was identified in up to 32% of the cells (Figure 3b, panel 3). About 10% of animals from the 470 line, which expressed the highest levels of mutant BRAF mRNA, developed melanoma; the median survival for this line was 295 days. In line 476, melanomas were rare, with a median survival of 595 days. Figure 3d shows the Kaplan–Meier survival curves for these lines generated in this study. The mortality of animals dying without tumors was largely due to CNS involvement. Supplementary Table 1 tabulates the tumor incidence for the strains, and the incidence in the genetic backgrounds discussed below.

We next sought to determine the contribution of endogenous murine Braf versus human mutant trans-genic BRAF to abnormal signaling in these melanomas. siRNA to both the murine transcript and the human mutant transcript was introduced into murine control melanocytes, a melanoma cell line derived from the 470 mice, and a human melanoma cell line. As shown in Figure 3c, and consistent with our results derived from non-neoplatic skin (Figure 1f), phosphorylation of ERK is inhibited only by human mutant siRNA in the cell lines derived from the transgenic 470 mice and human melanomas.

We examined the tumors arising in the mutant *BRAF* background for additional biochemical and genetic changes. Phospho-Erk was uniformly overexpressed in the melanomas; expression levels by IHC seemed higher than in transgenic melanocytes (compare Figures 2b, 2 and 3b, panel 4). This increase in pErk level parallels that seen in the transition from human nevi to melanoma and may not be solely due to mutant BRAF (Uribe *et al.*, 2006). pAkt was also uniformly strongly expressed in the murine melanomas compared with melanocytes (compare Figures 2b, panel 4 and 3b, panel 6). In human melanomas, the PI3K-AKT pathway is almost always activated in conjunction with the MAPK pathway, with activation of AKT through phosphoryla-tion in human melanomas conveying prognostic sig-nificance (Dai *et al.*, 2005). One mechanism for AKT activation is that melanomas frequently accompany BRAF activation with loss of PTEN (Wu *et al.*, 2003; Tsao *et al.*, 2004; Goel *et al.*, 2006). Additional mechanisms include NRAS mutation and AKT amplification (Dhawan *et al.*, 2002; Stahl *et al.*, 2004). None of the tumors that arose in these mice showed Pten loss by IHC (Figure 3b, panel 5), and no *Pten* or *Nras* mutations were detected by sequencing. Although the mechanism is not yet clear, our observations here support the hypothesis that activation of these pathways is necessary for melanoma development and progression.

Human sporadic melanomas occur with additional alterations in the $p16^{Ink4a}$-pRB pathway. Here immuno-histochemistry for $p16^{Ink4a}$ showed heterogeneous or total loss of $p16^{Ink4a}$ expression in melanomas compared with benign hyperplastic melanocytes (compare Figures 2b, panel 6 and 3b, panel 7), illustrating the complete loss of $p16^{Ink4a}$ expression by IHC. Multiplex PCR of this tumor DNA showed homozygous deletion of the entire *Cdkn2a* locus (Figure 3e), and this deletion included exon 2 and therefore resulted in both $p16^{Ink4a}$ and

p19^{Arf} loss. Of the six analysed tumors, a second tumor showed exon 2 and 3 homozygous deletion, and all six showed absent or reduced *p16 ^{Ink4a}* expression by IHC. No other *p16^{Ink4a}* mutations were detected by sequencing, and no *p53* mutations were detected. The loss of *p16^{Ink4a}* results in loss of senescent phenotype of neoplastic BRAF V600E melanocytes (Figure 3b, panel 9).

The observations above emphasize that almost universal alterations in the p16^{INK4A}-CDK4-RB and p14^{ARF}-p53 pathways accompany activation of signaling pathways in human melanomas. This occurs most frequently through concurrent loss of p16^{INK4A} and p14^{ARF} via mutation or deletion of the *Cdkna2a* locus, as observed in this model. In contrast, mutations in p53 are relatively rare in melanoma (Castresana *et al.*, 1993). The loss of the p14^{ARF} product of the *Cdkna2a* locus (Pomerantz *et al.*, 1998; Zhang *et al.*, 1998; Christophorou *et al.*, 2006) renders p53 mutation superfluous, as supported by cell line data, which show that most p53 mutations occur in melanoma when the *Cdkna2a* locus is normal (Haluska *et al.*, 2006). Still it has been shown that p53 loss contributes to the capacity of H-RAS to promote murine melanoma (Bardeesy *et al.*, 2001) and with mutant BRAF to promote zebra fish melanoma (Patton *et al.*, 2005). Thus, we also sought to test the hypotheses that the combination of mutant BRAF and an introduced deficiency for either *Cdkn2A* or *p53* would augment the development of melanomas.

Introduction of the mutant *BRAF* allele into *Cdkn2a*- and *p53*-deficient backgrounds leads to an increase in tumor incidence

Concentrating on the 470 and 476 lines, for which we had determined BRAF expression levels, we crossed these lines with *Cdkn2a*-null mice (Serrano *et al.*, 1996; Chin *et al.*, 1997) (a generous gift of Lynda Chin), which carry a deletion of *Cdkn2a* exons 2 and 3 and therefore abrogate both *p16^{Ink4a}* and *p19^{Arf}* expression, and with *p53*-null mice (Jackson Laboratory, Bar Harbor, ME, USA). Murine strains that carry *Cdkn2a* deletions develop a variety of tumors but fail to develop melanoma (Serrano *et al.*, 1996). Our results showed that the incidence of melanomas increased with *Cdkn2a* or *p53* deficiency, that the latency of tumor formation is markedly lessened, and that the lifespan of populations carrying these concurrent genetic defects is substantially reduced. Figure 4a (panel 1) illustrates metastatic melanoma in the lung arising in a transgenic *BRAF V600E Cdkn2a$^{+/-}$* background, with other mice also showing metastatic clusters of cells in the lymph nodes. Primary tumors as well as metastatic tumors showed loss of p16^{Ink4a} by IHC, retention of *Pten* expression and overexpression of *pAkt* (Figure 4b, panels 8, 5 and 4, respectively). Retained *p53* expression was found to have a strong cytoplasmic pattern (Figure 4b, panel 6). SA-*β*-gal expression is lost, consistent with abrogation of senescence (Figure 4b, panel 9). Results in the *p53*-deficient background were similar histopathologically and immunohistochemically (Supplementary Figure 4).

In the *Cdkn2a*-null background, which is deficient for both p16^{Ink4a} and p19^{Arf}, and which closely replicates the mutations seen in many human metastatic melanomas and melanoma cell lines, mortality was uniform and very early. Mice developed hydrocephalus and paralysis within days to weeks, as shown in Figure 4a, panel 2. Histology showed a pigmented cell proliferation within the CNS and especially the spinal cord, as seen in Figure 4a (panel 3), the result of which is obstruction of CNS outflow, hydrocephalus and death within 22–60 days (Supplementary Figure 3a, panel 2 and Figure 3b, panels 1–4, showing spinal cord tumors in BRAF *Cdkn2a$^{+/-}$*background).

We conclude that the BRAF-V600E mutation is not sufficient for tumor formation and loss of the *Cdkn2a* locus is a common and perhaps necessary step in the progression of tumor development in this background. This is not surprising, as the loss of *p16^{Ink4a}*, or the loss of *p53* and the predicted subsequent reduction in p21 both result in the deregulation of Cyclin

and CDK complexes and control of cellular proliferation. This also has a direct implication with relation to human melanoma genetics, and this mouse model faithfully recapitulates the human disease.

The understanding of the genetic changes contributing to the development of melanoma has been poorly exploited therapeutically. With the discovery of *BRAF* mutations in a large proportion of melanomas, our comprehension of the mechanistic steps giving rise to these tumors has been dramatically improved. Recent data shed light on the genetic alterations of a subset of tumors that do not carry BRAF mutations (Curtin *et al.,* 2005), but the most appealing therapeutic target remains mutated BRAF. Pharmacologic inhibition of the signaling intermediate BRAF by sorafenib alone does not lead to clinical responses (Eisen *et al.,* 2006), in contrast to inhibition in other tumor types of upstream signal-initiating molecules such as EGFR (Lynch *et al.,* 2004). This emphasizes the need for understanding concurrent genetic alterations that occur in melanoma development. The MAPK pathway is driven both by RAS and by BRAF in almost all cell types. In melanoma, RAS is mutated in <20% of cases, and usually mutation favors N-RAS. Two mouse models that carry alterations in the RAS signaling cascade and develop melanoma have been reported and studied. One is a murine model carrying activated H-RAS on a tyrosinase promoter. This model shows melanocytic hyperplasia with intense skin pigmentation. Placement of Tyr-RAS into a *Cdkn2a*- or *p53*-null background resulted in the development of highly vascularized but amelanotic melanoma and no metastases (Chin *et al.,* 1997). A second RAS mouse model is more faithful to human melanoma genetics: it carries the melanocytic expression of NRAS Q61K under the control of the tyrosinase promoter. Tyr-NRAS results in a hyperpig-mented skin phenotype and the formation of melanomas and favors the acquisition of a metastatic behavior on a *Cdkn2a* $^{-/-}$ background (Ackermann *et al.,* 2005). In our Tyr-BRAF mouse, metastatic melanoma develops both in the wild-type background and in *Cdkn2a*$^{+/-}$ background. Mutation in BRAF is probably serving as an early event favoring the initiation of melanoma, but because oncogenic BRAF induces senescence the melanocytes progress to nevi and require a second alteration in the genome to circumvent senescence and allow melanoma formation (Table 1).

On the basis of melanoma formation consequent to spontaneous or engineered loss of CDKN2a in combination with BRAF V600E expression in melanocytes, our mouse model is the first of its kind that recapitulates human melanoma with its genetic features. The precise nature of additional steps that occur as melanomas develop in the context of mutant BRAF, such as activation of AKT and the mechanisms that control them, is not yet understood. This mouse model will enable us to use genetic methods to understand this progression and to test putative therapeutic strategies *in vitro* and *in vivo*.

Materials and methods

Construction of transgenic mice

The *BRAF* transgene consisted of a 2.3-kb fragment of a *BRAF* V600E cDNA cloned from human melanoma cell line A375 by RT–PCR. The mouse tyrosinase enhancer, promoter and SV40 poly-A tail were generous gifts from Dr Louis Montilou (CNB, Spain). *BRAF* V600E was inserted downstream of the tyrosinase enhancer promoter and the SV40 poly-A tail was inserted downstream of *BRAF*. The DNA construct was gel purified (Gene Clean Turbo kit from Qbiogen, Carlsbad, CA, USA), sequenced and microinjected into single-cell embryos of F1 C57BL/J6XCBA mice. We identified the transgene-positive founder pups by Southern blot and PCR.

Southern blots

Purified genomic DNA of 20–30 μg obtained from tail biopsy was digested overnight with *Xba*I and *Kpn*I enzymes and Southern blotted with standard methods. Probe LCR1 was amplified from the tyrosinase enhancer region and cloned into a TA vector. The LCR1 fragment was digested and gel purified, and labeled randomly with a random primer kit (Amersham Biosciences, Piscataway, NJ, USA) using ^{32}P. The membrane was incubated with the radioactively labeled probe and washed by standard protocols. The membrane was exposed to an X-ray film at −80 ºC.

RT–PCR analysis

Total RNA was isolated from various major organs, such as the skin, heart, brain, lung, liver and spleen, using the Ribopure kit (Ambion, Austin, TX, USA). Total RNA was used for single-step RT–PCR with the Superscript one-step RT–PCR kit (Invitrogen, Carlsbad, CA, USA). The primer pair used for RT-PCR were; forward primer for the BRAF cDNA (5′-GGA TAC CTG TCT CCA GAT CTC AGT AAG-3′) and the reverse primer from the SV40 poly-A Tail (5′-TAG AAT GTT GAG AGT CAG CAG TAG CCT-3′). These primer pairs amplify two bands, one among them being 65 bp shorter, which represents the spliced 3′ untranslated intron. For real-time PCR the following primers (these are human BRAF specific primers) were used: BRAFRTU1 (5′-GTGGATGGCAACAGAAGTC-3′) and BRAFRTL1 (5′-GAAACCAGCCCGATTCAAGGA-3′). For internal control we use 18S rRNA primer sets (Ambion).

Histology and immunohistochemistry

Routine histology was carried out on 10% neutral buffered formalin-fixed tissues. For mouse brain, whole skull was fixed in Bouin's fixative for about 14–18 days. All immunohisto-chemistry was carried out on formalin-fixed paraffin-embedded 5-μm sections using standard protocols. Tissue sections were incubated at 4 ºC overnight with primary antibodies: pMapk antibody (cat#4376, 1:100; Cell Signaling, Danvers, MA, USA), pAkt (cat#3787, 1:50; Cell Signaling), S-100 (1:150; AbCam, Cambridge, MA, USA), Pten and p53 (1:100; ab23694 and ab32049, respectively, AbCam), Ki-67 (rabbit monoclonal clone Sp6, 1:250; Labvision, Fremont, CA, USA), except for $p16^{Ink4a}$ (1:100, F-12; Santa Cruz Biotechno-logy, Santa Cruz, CA, USA), which was incubated for 45 min at room temperature. A biotinylated goat anti-rabbit secondary antibody (1:200; Vector Laboratories, Burlingame, CA, USA) was incubated for 1 h at room temperature. For $p16^{Ink4a}$ staining we used the mouse on mouse tissue staining kit (Vector Laboratories) as recommended by the manufacturer. Avidin-biotin peroxidase complexes were then incubated for 30 min (Elite ABC reagent; Vector Laboratories). Nova-Red (Vector Laboratories) was used as the final chromogen and hematoxylin was used as the nuclear counter stain. Staining for SA-*β*-gal was carried out as described (Dimri *et al.*, 1995) on fresh frozen skin samples from both wild-type and BRAF transgenic animal.

Isolation of primary epidermal melanocytes and siRNA transfection

Epidermal melanocytes were harvested from 1-day-old pups as described earlier (Tamura *et al.*, 1987). For siRNA transfection studies we harvested about 2×10^6 melanocytes (about 16–18 days-old culture) and transfected them with 100 pmol of siRNA targeting either human *BRAF* V600E (stealth siRNA synthesized from Invitrogen) or mouse BRAF (Dharmacon, Lafayette, CO, USA) using nucleofection technology (NHEM kit from Amaxa Biosystem, Cologne, Germany). As a control, we used Medium GC content negative-control siRNA obtained from Invitrogen. To control transfection efficiency we used GFP plasmid vector. For controls we used BIOBR wild-type melanocytes (Tamura *et al.*, 1987; Yale University, Yale, CT, USA). At 48 h after siRNA transfection the whole cell protein was

harvested. The total protein was estimated using DC protein assay reagent (Bio-Rad, Hercules, CA, USA). In all, 20 μg of total protein was loaded onto 4–12% Bis–Tris Gel (Invitrogen) and run in 1 × MOPS buffer. The protein was transferred to nitrocellulose membrane (Invitrogen) and western blotting was carried outusing BRAF antibody (cat# sc-55522, 1:4000; Santa Cruz), pERK1/2 (cat# 9101, 1:1000; Cell Signaling), total ERK (cat# 4695, 1:1000; Cell Signaling), pMek1/2 (cat#9121, 1:1000; Cell Signaling), total Mek (cat# 9122, 1:1000; Cell Signaling) and β-actin (1:6000; Sigma Aldrich, St Louis, MO, USA). The sequence of *BRAF* V600E specific siRNA used was as published earlier, using sense strand GGUCUAGCU ACAGAGAAAUCUCGAU (Hingorani *et al.*, 2003; Sharma *et al.*, 2005) and mouse *Braf*-specific siRNA sense strand GGAGUUACAUGUUGAAGUAUU (Dharmacon).

Supplementary Material

Refer to Web version on PubMed Central for supplementary material.

Acknowledgments

This work was supported by NIH grant CA095798 to FGH. We thank Mohammad Miri for technical assistance, Dr Louis Montoliu for the tyrosinase promoter, Dr Lynda Chin for the mouse strains, and Dr Philip Tsichlis and Dr Trevor Pemberton for useful discussions.

References

Ackermann J, Frutschi M, Kaloulis K, McKee T, Trumpp A, Beermann F. Metastasizing melanoma formation caused by expression of activated N-RasQ61K on an INK4a-deficient background. Cancer Res. 2005; 65:4005–4011. [PubMed: 15899789]

Bardeesy N, Bastian BC, Hezel A, Pinkel D, DePinho RA, Chin L. Dual inactivation of RB and p53 pathways in RAS-induced melanomas. Mol Cell Biol. 2001; 21:2144–2153. [PubMed: 11238948]

Castresana JS, Rubio MP, Vasquez JJ, Idoate M, Sober AJ, Seizinger BR, et al. Lack of allelic deletion and point mutation as mechanisms of p53 activation in human malignant melanoma. Int J Cancer. 1993; 55:562–565. [PubMed: 8104906]

Chang DL, Qiu W, Ying H, Zhang Y, Chen CY, Xiao ZX. ARF promotes accumulation of retinoblastoma protein through inhibition of MDM2. Oncogene. 2007; 26:4627–4634. [PubMed: 17297463]

Chin L, Pomerantz J, Polsky D, Jacobson M, Cohen C, Cordon-Cardo C, et al. Cooperative effects of INK4a and ras in melanoma susceptibility *in vivo*. Genes Dev. 1997; 11:2822–2834. [PubMed: 9353252]

Christophorou MA, Ringshausen I, Finch AJ, Swigart LB, Evan GI. The pathological response to DNA damage does not contribute to p53-mediated tumour suppression. Nature. 2006; 443:214–217. [PubMed: 16957739]

Courtois-Cox S, Genther Williams SM, Reczek EE, Johnson BW, McGillicuddy LT, Johannessen CM, et al. A negative feedback signaling network underlies oncogene-induced senescence. Cancer Cell. 2006; 10:459–472. [PubMed: 17157787]

Curtin JA, Fridlyand J, Kageshita T, Patel HN, Busam KJ, Kutzner H, et al. Distinct sets of genetic alterations in melanoma. N Engl J Med. 2005; 353:2135–2147. [PubMed: 16291983]

Dai DL, Martinka M, Li G. Prognostic significance of activated Akt expression in melanoma: a clinicopathologic study of 292 cases. J Clin Oncol. 2005; 23:1473–1482. [PubMed: 15735123]

Dhawan P, Singh AB, Ellis DL, Richmond A. Constitutive activation of Akt/protein kinase B in melanoma leads to up-regulation of nuclear factor-kappaB and tumor progression. Cancer Res. 2002; 62:7335–7342. [PubMed: 12499277]

Dimri GP, Lee X, Basile G, Acosta M, Scott G, Roskelley C, et al. A biomarker that identifies senescent human cells in culture and in aging skin *in vivo*. Proc Natl Acad Sci USA. 1995; 92:9363–9367. [PubMed: 7568133]

Eisen T, Ahmad T, Flaherty KT, Gore M, Kaye S, Marais R, et al. Sorafenib in advanced melanoma: a phase II randomised discontinuation trial analysis. Br J Cancer. 2006; 95:581–586. [PubMed: 16880785]

Goel VK, Lazar AJ, Warneke CL, Redston MS, Haluska FG. Examination of mutations in BRAF, NRAS, and PTEN in primary cutaneous melanoma. J Invest Dermatol. 2006; 126:154–160. [PubMed: 16417231]

Gray-Schopfer VC, Cheong SC, Chong H, Chow J, Moss T, Abdel-Malek ZA, et al. Cellular senescence in naevi and immortalisation in melanoma: a role for p16? Br J Cancer. 2006; 95:496–505. [PubMed: 16880792]

Haluska FG, Tsao H, Wu H, Haluska FS, Lazar A, Goel V. Genetic alterations in signaling pathways in melanoma. Clin Cancer Res. 2006; 12:2301s–2307s. [PubMed: 16609049]

Hingorani SR, Jacobetz MA, Robertson GP, Herlyn M, Tuveson DA. Suppression of BRAF(V599E) in human melanoma abrogates transformation. Cancer Res. 2003; 63:5198–5202. [PubMed: 14500344]

Laud K, Marian C, Avril MF, Barrois M, Chompret A, Goldstein AM, et al. Comprehensive analysis of CDKN2A (p16INK4A/p14ARF) and CDKN2B genes in 53 melanoma index cases considered to be at heightened risk of melanoma. J Med Genet. 2006; 43:39–47. [PubMed: 15937071]

Lynch TJ, Bell DW, Sordella R, Gurubhagavatula S, Okimoto RA, Brannigan BW, et al. Activating mutations in the epidermal growth factor receptor underlying responsiveness of non-small-cell lung cancer to gefitinib. N Engl J Med. 2004; 350:2129–2139. [PubMed: 15118073]

Michaloglou C, Vredeveld LC, Soengas MS, Denoyelle C, Kuilman T, van der Horst CM, et al. BRAFE600-associated senescence-like cell cycle arrest of human naevi. Nature. 2005; 436:720–724. [PubMed: 16079850]

Muthusamy V, Hobbs C, Nogueira C, Cordon-Cardo C, McKee PH, Chin L, et al. Amplification of CDK4 and MDM2 in malignant melanoma. Genes Chromosomes Cancer. 2006; 45:447–454. [PubMed: 16419059]

Patton EE, Widlund HR, Kutok JL, Kopani KR, Amatruda JF, Murphey RD, et al. BRAF mutations are sufficient to promote nevi formation and cooperate with p53 in the genesis of melanoma. Curr Biol. 2005; 15:249–254. [PubMed: 15694309]

Pollock PM, Harper UL, Hansen KS, Yudt LM, Stark M, Robbins CM, et al. High frequency of BRAF mutations in nevi. Nat Genet. 2003; 33:19–20. [PubMed: 12447372]

Pollock PM, Meltzer PS. A genome-based strategy uncovers frequent BRAF mutations in melanoma. Cancer Cell. 2002; 2:5–7. [PubMed: 12150818]

Pomerantz J, Schreiber-Agus N, Liegeois NJ, Silverman A, Alland L, Chin L, et al. The Ink4a tumor suppressor gene product, p19Arf, interacts with MDM2 and neutralizes MDM2's inhibition of p53. Cell. 1998; 92:713–723. [PubMed: 9529248]

Serrano M, Lee H, Chin L, Cordon-Cardo C, Beach D, DePinho RA. Role of the INK4a locus in tumor suppression and cell mortality. Cell. 1996; 85:27–37. [PubMed: 8620534]

Sharma A, Trivedi NR, Zimmerman MA, Tuveson DA, Smith CD, Robertson GP. Mutant V599EB-Raf regulates growth and vascular development of malignant melanoma tumors. Cancer Res. 2005; 65:2412–2421. [PubMed: 15781657]

Sharpless NE, Kannan K, Xu J, Bosenberg MW, Chin L. Both products of the mouse Ink4a/Arf locus suppress melanoma formation *in vivo*. Oncogene. 2003; 22:5055–5059. [PubMed: 12902988]

Stahl JM, Sharma A, Cheung M, Zimmerman M, Cheng JQ, Bosenberg MW, et al. Deregulated Akt3 activity promotes development of malignant melanoma. Cancer Res. 2004; 64:7002–7010. [PubMed: 15466193]

Sviderskaya EV, Hill SP, Evans-Whipp TJ, Chin L, Orlow SJ, Easty DJ, et al. p16(Ink4a) in melanocyte senescence and differentiation. J Natl Cancer Inst. 2002; 94:446–454. [PubMed: 11904317]

Tamura A, Halaban R, Moellmann G, Cowan JM, Lerner MR, Lerner AB. Normal murine melanocytes in culture. in vitro Cell Dev Biol. 1987; 23:519–522. [PubMed: 3610949]

Tief K, Schmidt A, Beermann F. New evidence for presence of tyrosinase in substantia nigra, forebrain and midbrain. Brain Res Mol Brain Res. 1998; 53:307–310. [PubMed: 9473705]

Tonks ID, Nurcombe V, Paterson C, Zournazi A, Prather C, Mould AW, et al. Tyrosinase-Cre mice for tissue-specific gene ablation in neural crest and neuroepithelial-derived tissues. Genesis. 2003; 37:131–138. [PubMed: 14595836]

Tsao H, Goel V, Wu H, Yang G, Haluska FG. Genetic interaction between NRAS and BRAF mutations and PTEN/MMAC1 inactivation in melanoma. J Invest Dermatol. 2004; 122:337–341. [PubMed: 15009714]

Uribe P, Andrade L, Gonzalez S. Lack of association between BRAF mutation and MAPK ERK activation in melanocytic nevi. J Invest Dermatol. 2006; 126:161–166. [PubMed: 16417232]

Wu H, Goel V, Haluska FG. PTEN signaling pathways in melanoma. Oncogene. 2003; 22:3113–3122. [PubMed: 12789288]

Zhang Y, Xiong Y, Yarbrough WG. ARF promotes MDM2 degradation and stabilizes p53: ARF-INK4a locus deletion impairs both the Rb and p53 tumor suppression pathways. Cell. 1998; 92:725–734. [PubMed: 9529249]

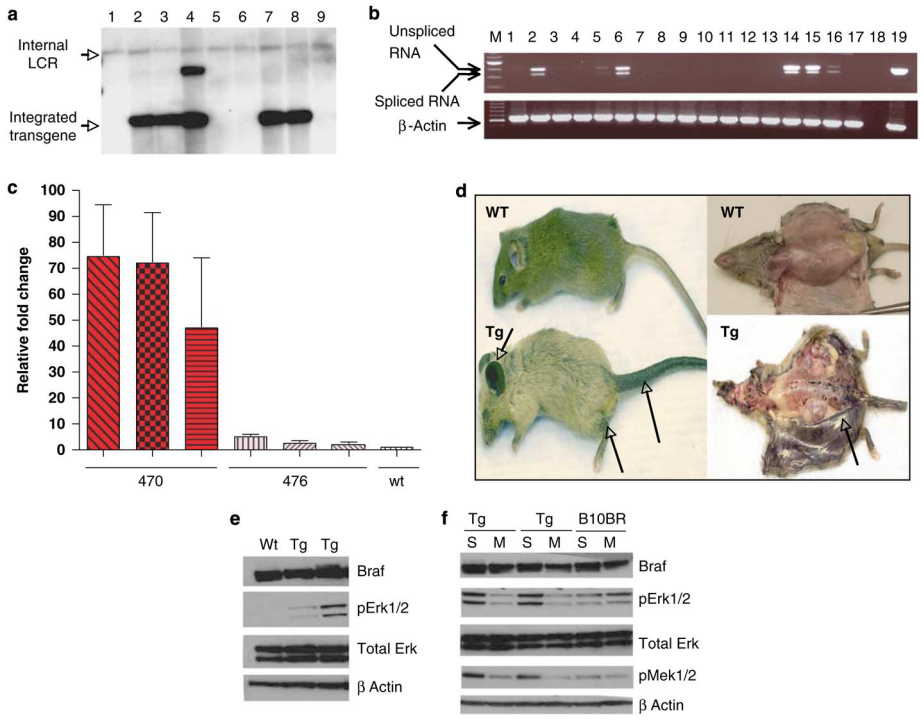

Figure 1.

Genotype and phenotype of the mutant *BRAF* transgenic mouse. (**a**) Southern blot detection of transgene. A strong extra band in lane 4 might be because of partial digestion of genomic DNA. LCR, locus control region (part of tyrosinase enhancer). (**b**) RT–PCR analysis of BRAF expression. The bands of 500 and 435 bp represent unspliced and spliced mRNA, respectively. The spliced form represents about 65 bp of 3′ untranslated intron, which is about 65 bp in size. 1–6, tissues from *BRAF* V600E mice: 1, heart; 2, brain; 3, kidney; 4, liver; 5, lung; 6, skin. 7–13, corresponding tissues from C57BL6 animal. 14–16, transgenic isolated melanocytes. 17, wild-type melanocytes. 18, negative control. 19 DNA vector (not spliced). Lower panel, β-actin controls; 19, positive control ACTB. (**c**) Real-time RT-PCR quantitative expression analysis of *BRAF* V600E expression. Three whole-skin samples from 470 animals, three from 476, and wild type (wt). Each analysis was carried out in triplicate. (**d**) Phenotype of *BRAF* V600E Tg mouse line 470 compared with C57BL6. (**e**) Western blot of whole-cell lysate from cultured melanocytes of wt and transgenic (Tg) animals. (**f**) Western blot of the effect of human *BRAF* V600E region-specific siRNA on mouse melanocytes from *BRAF* V600E Tg mice and B10BR wt mouse melanocyte cell lines. S: scrambled (irrelevant) siRNA, M: BRAF *V600E* mutant region-specific siRNA. pErk1/2 is significantly and specifically decreased by human *BRAF* V600E specific siRNA as compared with control. pMek is also decreased.

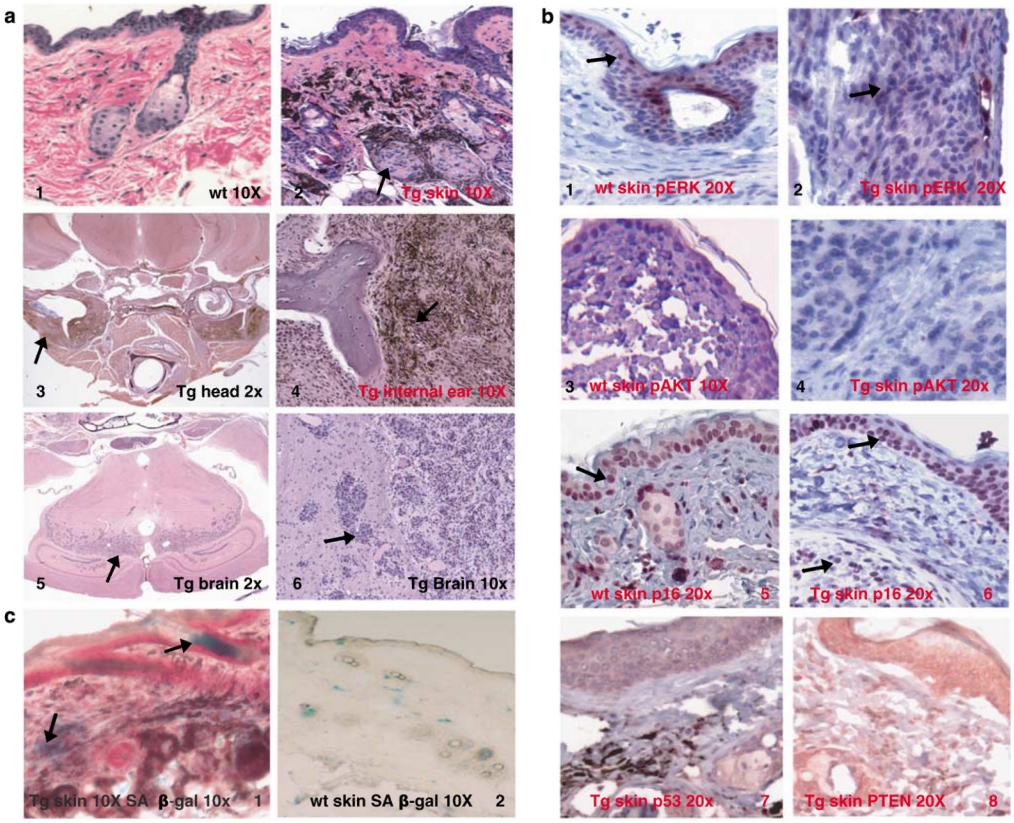

Figure 2.

Histopathology and biochemistry of transgenic animals. (**a**) Panel 1, H&E of skin of wild-type animal; panel 2, H&E of skin of *BRAF* V600E animal (line 470) showing dermal melanocytic proliferations. Panel 3, section through the base of the skull showing vestibular schwannian melanocytic tumors, which are shown in high magnification in panel 4. Panel 5, the midbrain showing melanocytic infiltration. Panel 6, high-magnification image of the same tumor (all sections from line 470). (**b**) Immunohistochemistry of wild-type skin (panels 1, 3 and 5) and Tg skin (line 470, panels 2, 4 and 6) are for pErk, pAkt and $p16^{Ink4a}$, whereas panels 7 and 8 are staining for p53 and PTEN, respectively, in the skin of line 470. (**c**), SA-β-gal is induced in the skin of *BRAF* V600E (line 470, panel 1) animals as compared with wild-type skin (panel 2), which is consistent with a senescent response to mutant BRAF.

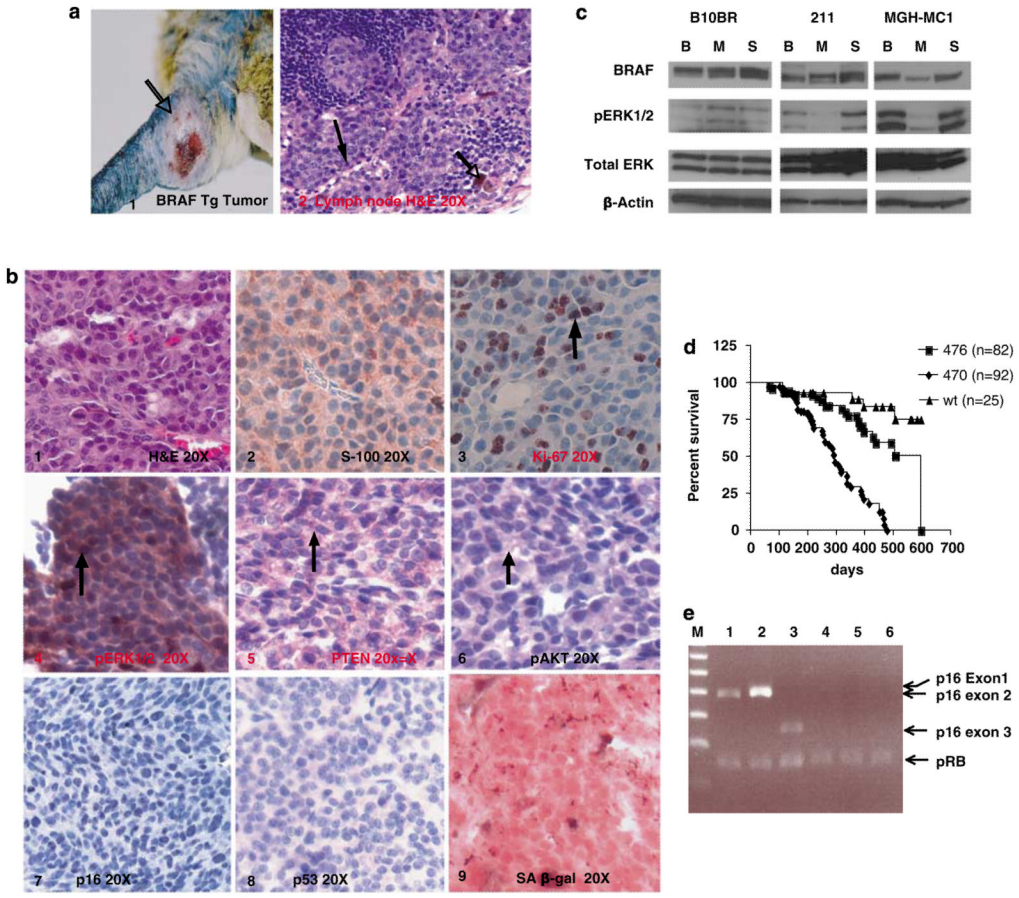

Figure 3.

Melanomas in mice carrying mutant *BRAF* alone metastasize and show pAkt activation and loss of the Ink4a locus. (**a**) Phenotype of Tg mouse melanoma tumor, and histology of a metastasis to a draining lymph node (line 470). (**b**) Immunohistochemistry of one of the representative melanomas from *BRAF* V600E Tg mice. Panel 1, H&E; 2, S100; 3, Ki-67; 4, pErk; 5, Pten; 6, pAkt; 7, p16; 8, p53; 9, SA-β-gal. (**c**) Specificity of signaling alterations to mutant BRAF activity. B10BR, wild-type mouse melanocyte cell line; 211, tumor cell line derived from *BRAF V600E* mouse melanoma; MGH-MC1, human melanoma cell line carrying *BRAF* V600E mutation; B: mouse BRAF-specific siRNA; M: human *BRAF* V600E-specific siRNA; S: luciferase (irrelevant) siRNA. pErk level was significantly and specifically downregulated by human *BRAF* V600E specific siRNA as compared with mouse Braf siRNA. (**d**) Kaplan–Meier plot of mortality of *BRAF* V600E transgenic lines. (**e**) Multiplex PCR of *Cdkn2a* exons 1α, 2 and 3 in control and in tumor from *BRAF* V600E animal. Lower band in all lanes, pRb control. Lanes 1–3 contain tail DNA and lanes 4–6 contain DNA from tumor sample #211. Lanes 1 and 4, exon 1α; 2 and 5, exon 2; 3 and 6, exon 3.

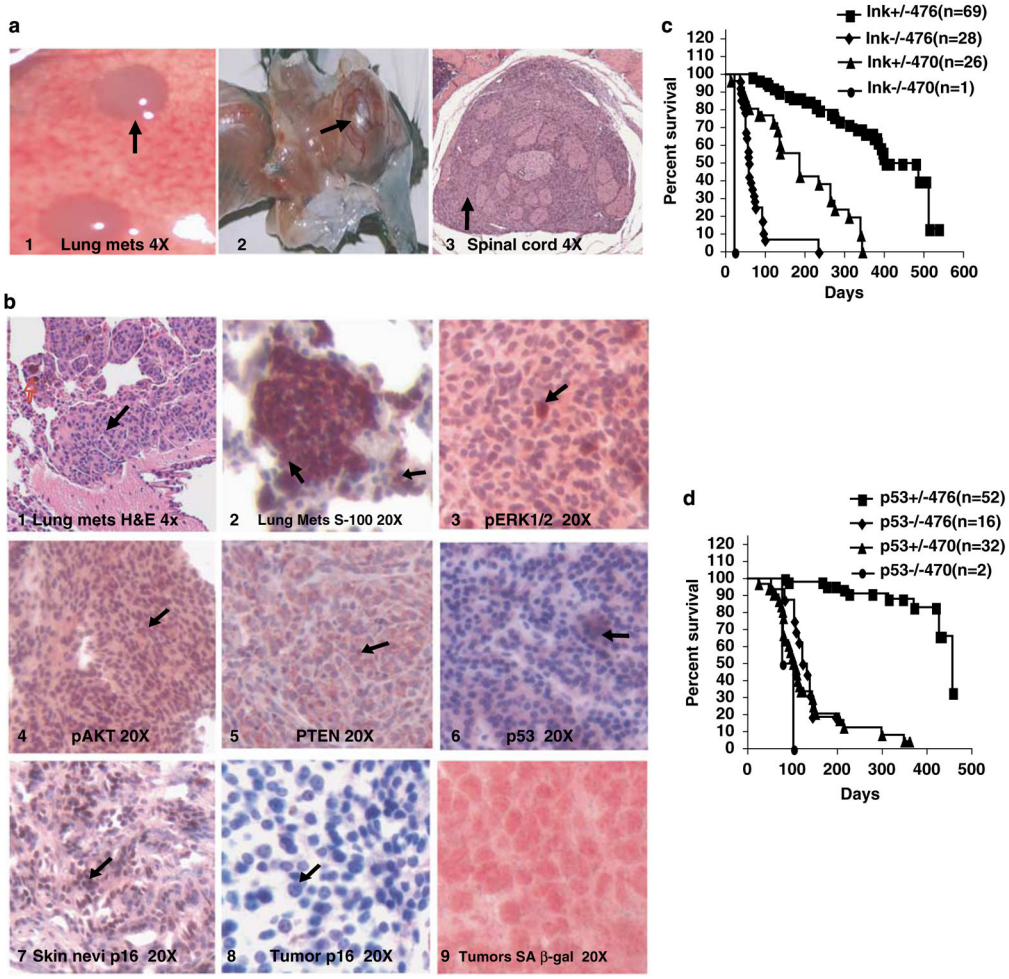

Figure 4.

Melanomas in *Cdkn2a*- and p53-deficient mice show the Ink4a locus and abrogation of senescence. (**a**) Panel 1, lung metastases in a tumor from *BRAF* V600E (470) × *Cdkn2a*$^{+/-}$ animal; 2, hydrocephalus in the same genotype; 3, spinal cord transverse section showing melanocytic infiltration of spinal cord. (**b**) Immunohistochemistry of primary melanoma arising in *BRAF* V600E × *Cdkn2a*$^{+/-}$ animal. Panel 1, pErk; 2, pAkt; 3, Pten; 4, skin p16^{Ink4a}; 5, tumor p16^{Ink4a}; 6, p53; 7 and 8, p16 and 9, SA-B-gal senescence staining on one of the BRAF+*Cdkn2a* tumors. (**c**) Kaplan–Meier plot of *Cdkn2a* crosses showing the relationship of mortality to mutant *BRAF* dose and inversely to *Cdkn2a* dose. (**d**) Similar plot of p53 crosses.

Table 1

Changes that occur during progression of melanocytes to melanoma

	Melanocyte	Human nevus/Tg Braf model	Melanoma
BRAF status	Normal	V600E	V600E
pERK level	Low	Moderately increased	High
pAKT level	Low	Low	High
p16 expression	Low	Induced	Lost
SA-B-gal expression	Low	Induced	Lost
Phenotype	Quiescent	Senescent	Malignant